Structural Health Monitoring

Compressive sensing of wireless sensors based on group sparse optimization for structural health monitoring

Journal:	*Structural Health Monitoring*
Manuscript ID	Draft
Manuscript Type:	Original Manuscript
Date Submitted by the Author:	n/a
Complete List of Authors:	Bao, Yuequan; Harbin Institute of Technology, School of Civil Engineering Shi, Zuoqiang; Tsinghua University, Mathematical Sciences Center Wang, Xiaoyu; Harbin Institute of Technology, School of Civil Engineering Li, Hui; Harbin Institute of Technology, School of Civil Engineering
Keywords:	Structural health monitoring, compressive sensing, data reconstruction, group sparse optimization, wireless sensor
Abstract:	Vibration signals of most civil infrastructures have sparse characteristic, (i.e., only a few modes contribute to the vibration of the structures). Therefore, the vibration data usually have sparse representation. Additionally, the measured vibration data by the sensors placed on different locations of structure almost has the same sparse structure in the frequency domain. Based on the group sparsity of the structural vibration data, a group sparse optimization algorithm based compressive sensing (CS) for wireless sensors are proposed. Different from the Nyquist sampling theorem, the data is first acquired by a non-uniform low rate random sampling method according to the CS theory. Then, the group sparse optimization algorithm is developed to reconstruct the original data from incomplete measurements. The field test on Xiamen Haicang Bridge with wireless sensors is carried out to illustrate the effectiveness of the proposed approach. The results show that the smaller reconstruction errors can be achieved by using multiple sensors data with the group sparse optimization method than only using single sensor data. Even using only 10% random sampling data, the original data can be reconstructed by the group sparse optimization method with small reconstruction error. In addition, the modal parameters can also be identified from the reconstruction data with small identification errors.

Compressive sensing of wireless sensors based on group sparse optimization for structural health monitoring

Yuequan Bao[1, 2], Zuoqiang Shi[3], Xiaoyu Wang[1, 2], Hui Li[1, 2*]

[1]*Key Lab of Structures Dynamic Behavior and Control of the Ministry of Education (Harbin Institute of Technology), Harbin, 150090, China*

[2]*School of Civil Engineering, Harbin Institute of Technology, Harbin China, 150090*

[3]*Mathematical Sciences Center, Tsinghua University, Beijing, China, 100084*

Abstract

Vibration signals of most civil infrastructures have sparse characteristic, (i.e., only a few modes contribute to the vibration of the structures). Therefore, the vibration data usually have sparse representation. Additionally, the measured vibration data by the sensors placed on different locations of structure almost has the same sparse structure in the frequency domain. Based on the group sparsity of the structural vibration data, a group sparse optimization algorithm based compressive sensing (CS) for wireless sensors are proposed. Different from the Nyquist sampling theorem, the data is first acquired by a non-uniform low rate random sampling method according to the CS theory. Then, the group sparse optimization algorithm is developed to reconstruct the original data from incomplete measurements. The field test on Xiamen Haicang Bridge with wireless sensors is carried out to illustrate the effectiveness of the proposed approach. The results show that the smaller reconstruction errors can be achieved by using multiple sensors data with the group sparse optimization method than only using single sensor data. Even using only 10% random sampling data, the original data can be reconstructed by the group sparse optimization method with small reconstruction error. In addition, the modal parameters can also be identified from the reconstruction data with small identification errors.

Keywords: Structural health monitoring; compressive sensing; data reconstruction; group sparse optimization; wireless sensor

* Corresponding Author
Email: lihui@hit.edu.cn (Hui Li). *Tel. & Fax: 86-451-8628-2013*

1 Introduction

1.1 Wireless sensors and sensor networks for SHM

The structural health monitoring (SHM) technology has already been developed several decades and a lot of civil infrastructures have been installed with some SHM systems all over world.[1-4] In the wired sensors based SHM system, the wired connection between sensors and data acquisition system reduces the reliability of SHM system, increases the system cost, and causes great difficulties for the maintenance and replacement. As reported, the wired monitoring system on the Bill Emerson Memorial Bridge in Cape Girardeau, Missouri, USA, costed more than $15,000 per sensor,[5] and a large portion of that cost is related to the wired data transmission cables. Wireless sensors and wireless network have intelligent data processing capabilities with embedding algorithm and does not have cables which will great reduce the sensor installation cost. In comparison with the traditional wired sensor monitoring systems, wireless sensors and wireless network possess several advantages that make them an attractive alternative for monitoring large civil infrastructure.

In SHM, great efforts have been made to explore wireless sensing systems. Some academic and commercial smart sensor prototypes have been developed and used in the field of SHM.[6-13] Straser and Kiremidjian[6] first developed smart wireless sensors for application to civil engineering structures. A more exhaustive review is given in reference.[7-8] Recently, wireless sensors have been used on many bridges for SHM purposes. On Jindo Bridge, a cable stayed bridge in Korea, 70 Imote2 smart wireless sensors has been installed for SHM.[9] On Geumdang Bridge, a continuous beam bridge, 28 wireless sensors has also been installed by Lynch et al. for SHM.[10] The Stork Bridge in Switzerland,[11] Ferriby Road Bridge in England, [12] and Rock Island Arsenal Government Bridge in USA[13] are all in-stalled with some wireless sensor based-SHM system.

Comparing with wired sensors, the wireless sensor and sensor networks need additional energy acquisition technology to ensure the power supply of sensor. In addition, in the long-term monitoring of the structure, the large amounts of data acquisition and wireless transmission are likely to cause the instability of wireless sensor network. The wireless data transmission process will consume most of the energy of sensor battery. Therefore, it is necessary for embed data compression algorithm to reduce the amount of data transmission as much as possible to minimize energy consumption,

prolonging the service life of wireless sensor. However, traditional data compression method, based on the sampling theorem, has its limitations: first complete collection of data, and then the data is compressed. For wireless sensor, data compression process will consume part of the energy. Therefore, new data compression methods are needed to effectively improve the wireless sensors and wireless sensor network for long-term SHM.

1.2 Compressive sensing for wireless sensors and SHM

To avoid the information loss when uniformly sampling a signal, the Shannon-Nyquist sampling theorem requires the sampling frequency at least two times of the signal's bandwidth. For the signal with high frequency, long term real time SHM with uniform sampling will produce large volume of data and result in high cost of data sampling, storage and transmission.

Compressive sensing (CS) provides a new sampling theory to reduce data acquisition with non-uniform low rate random sampling method, which said that the sparse or compressible signals can be exactly reconstructed from highly underdetermined sets of measurements under the assumption of signal sparsity and under certain conditions on the measurement matrix.[14-15] The potential of CS for the SHM has been investigated widely and many applications of CS have been presented. Bao et al.[16] investigated the CS for acceleration data collection of SHM, finding that the sparsity of the vibration acceleration response data of structures is the main factor that affects the data reconstruction accuracy. Mascarenas et al. [17] studied the compressed sensing techniques to detect damage in structures. In their research, the compressed sensor is first developed for collecting compressed coefficients from measurements and sending them to an off-board processor for signal reconstruction using l_1 norm minimization; then a compressed version of the matched filter is implemented on-board the sensor node for detecting structural damage. Peckens and Lynch [18] proposed a bio-inspired CS technique to acquire the data for SHM. O'Connor et al. [19] explored CS to reduce power consumption in wireless sensors for SHM. They modified the wireless sensor node to perform random sampling of data according to CS theory. Then, the random sampled data is transmitted off-site to a computational server for data reconstruction using the CoSaMP matching pursuit recovery algorithm and further processed for extraction of the structure's mode shapes. Bao et al [20] explored the use of CS to recover the lost data of wireless sensors for SHM, in which the random lost data are equivalent as compressed

data of CS and these lost data are reconstructed using the sparse optimization method with high accuracy. Furthermore, they embedded the CS based algorithm into Imote2 wireless sensor using a random demodulator technique; the field test results on the Songpu Bridge in Harbin, China showed the successful of the CS-based data loss recovery.[21]

Not only for data acquisition, CS method also explored to structural modal identification, structural damage identification and loads identification. Park et al.[22] proposed a novel method for modal identification directly using compressed sensing measurements. Yang and Nagarajaiah[23] proposed an output-only modal identification method combined with blind source separation (BSS) techniques and CS. In this method, the non-uniform low-rate random samples are directly used for modal identification. Wang and Hao[24] proposed a new CS-based damage identification scheme by regarding damage identification problems as pattern classification problems. Based on the sparsity symposium of structural damage, the l_1 sparse optimization methods of CS theory are also used for structural damage identification.[25-27] In additional, Bao et al.[28] presented a sparse optimization of CS theory-based approach for identification of distribution of moving heavy vehicle loads on cable-stayed bridges.

In SHM, most vibration signals of civil infrastructures not only have sparse characteristic, the measured vibration data at different locations of structure also has very similar sparse structure in the frequency domain. This property is called as group sparsity in this paper. To further increase the data reconstruction accuracy of CS in SHM, the group sparsity of multiple sensors data are explored to form a group sparse optimization method for high accuracy reconstruction of compressive sampling data by wireless sensor. The group sparsity has been exploited a lot in different areas. It has different names in different applications, for instance joint sparsity,[29,30] simultaneous sparse[31,32] group LASSO[33] et.al. In this paper, using the special structure of the Fourier basis, we develop an efficient algorithm based on the Augmented Lagrange Multiplier (ALM) method. In this algorithm, only Fast Fourier transform (FFT) or soft shrinkage is involved, so it is very efficient. The details of the algorithm is given in Section 2.

2 Compressive sensing based on group sparse optimization algorithm

2.1 Principle of the method

Different from the traditional Nyquist uniform sampling, the CS enables non-uniform low rate random sampling as shown in Figure 1. The Nyquist sampling needs to sense N samples of a signal to avoid information loss as shown in Figure 1(a); however, CS randomly sense much fewer $M \ll N$ as shown in Figure 1(b). According to the CS theory, if the original signal is sparse, CS is able to exactly recover it from far fewer incoherent random measurements than what is required by Shannon sampling theorem.

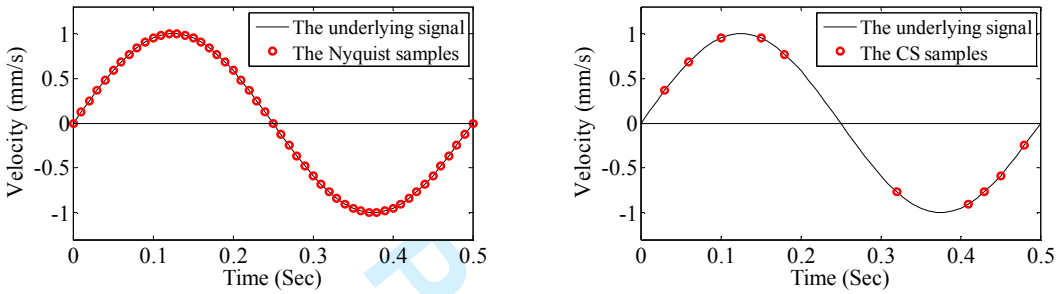

(a) Nyquist samples (b) CS samples

Figure 1. Nyquist sampling and CS sampling

Suppose that there are K sensors which are implemented in the structure. The acceleration is measured at discrete time t_j, $j=1,\ldots,M$ by each sensor. Here, we assume the entire time span of samples is $[0,T]$ and the sample time is uniformly distributed, i.e. $t_j = jT/M$, $j=1,\ldots,M$. By collecting all the data together, we get a $M\times K$ matrix, $\mathbf{U}$,

$$\mathbf{U} = \begin{bmatrix} u_{11} & u_{12} & \cdots & u_{1K} \\ u_{21} & u_{22} & \cdots & u_{2K} \\ \vdots & \vdots & \ddots & \vdots \\ u_{N1} & u_{N2} & \cdots & u_{NK} \end{bmatrix} \tag{1}$$

where u_{mk} is the data measured by the kth sensor at time t_m.

Then, the signal matrix, $\mathbf{U}$ is usually an incomplete matrix. Let $\boldsymbol{\Omega} = \{(m,k) : U_{m,k} \text{ is available}\}$ and $P_\Omega : R^{M\times K} \to R^{M\times K}$ is the zero padding operator, that is $\mathbf{Y} = P_\Omega \mathbf{U}$,

$$y_{m,k}=\begin{cases}u_{m,k}, & (m,k)\in\Omega\\ 0, & \text{otherwise}\end{cases} \tag{2}$$

Then the problem we are facing is how to calculate the original signal matrix $\mathbf{U}$ from the given signal $\mathbf{Y}=P_\Omega\mathbf{U}\in R^{M\times K}$.

The signal matrix $\mathbf{U}$ can be represented as

$$\mathbf{U}=\mathbf{\Psi X} \tag{3}$$

where $\mathbf{\Psi}$ is a Fourier matrix

$$\mathbf{\Psi}=\begin{bmatrix} e^{i2\pi t_1/T} & e^{i4\pi t_1/T} & \cdots & e^{i2M\pi t_1/T}\\ e^{i2\pi t_2/T} & e^{i4\pi t_2/T} & \cdots & e^{i2M\pi t_2/T}\\ \vdots & \vdots & \ddots & \vdots\\ e^{i2\pi t_M/T} & e^{i4\pi t_M/T} & \cdots & e^{i2M\pi t_M/T}\end{bmatrix} \tag{4}$$

where $\mathbf{X}\in C^{M\times K}$ are the Fourier coefficients of original signal that only have a few nonzero rows. This representation gives us an alternative way to recover the signal matrix $\mathbf{U}$, which is so called joint sparsity.

Considering the measurement noise, Eq. (3) is changed to

$$\mathbf{U}=\mathbf{\Psi X}+\boldsymbol{\varepsilon} \tag{5}$$

where $\boldsymbol{\varepsilon}\in R^{M\times K}$ is Gaussian noise matrix.

To take advantage of the joint sparsity, usually, we aim at minimizing the $\|\cdot\|_{p,q}$ norm of $\mathbf{X}\in R^{M\times K}$, where

$$\|\mathbf{X}\|_{p,q}=\left(\sum_{m=1}^{M}\|\mathbf{x}_m\|_p^q\right)^{1/q} \tag{6}$$

One of the most possible choice of p, q is $p=2$, $p=1$, and these values are also used in this paper. Then, the Fourier coefficients matrix $\mathbf{X}$ is recovered by solving the following optimization problem:

$$\min_{\mathbf{X}\in C^{M\times K}}\|\mathbf{X}\|_{2,1}+\frac{\mu}{2}\|P_\Omega(\mathbf{\Psi X})-P_\Omega\mathbf{U}\|_2^2 \tag{7}$$

Once the optimal solution $\mathbf{X}_{rec}$ is obtained, the recovered signal matrix is given by

$$\mathbf{U}_{rec}=\mathbf{\Psi X}_{rec} \tag{8}$$

2.2 Algorithm

In this section, we give an iterative algorithm to solve the optimization problem of Eq. (7). First, we rewrite Eq. (7) as follows:

$$\min_{\substack{\mathbf{X}\in R^{M\times K},\\ \mathbf{Z}\in R^{M\times K}}} \|\mathbf{X}\|_{2,1}+\frac{\mu}{2}\|\mathbf{Z}\|_2^2, \text{ subject to: } \mathbf{Z}=\mathbf{\Psi X}\text{-}P_{\Omega}\mathbf{U} \tag{9}$$

We use the augmented Lagrange multiplier (ALM) algorithm to solve Eq. (9). The ALM algorithm solves a constrained problem by iteratively solving a sequence of unconstrained problem. For a general constrained optimization problem

$$\min F(x), \text{ subject to: } g(x)=0 \tag{10}$$

ALM algorithm solves it by the following iterative process:

- $x^k=\arg\min_x F(x)+\frac{\tau}{2}\left\|g(x)+\omega^k/\tau\right\|_2^2$
- $\omega^{k+1}=\omega^k+\tau g\left(x^k\right)$

where τ is a parameter in ALM. It is well known that the convergence of ALM algorithm is robust to the choice of this parameter.

Applying ALM algorithm to Eq. (9), we get an iterative algorithm

$$\left(\mathbf{X}^{k+1},\mathbf{Z}^{k+1}\right)=\arg\min_{\substack{\mathbf{X}\in C^{M\times K},\\ \mathbf{Z}\in R^{M\times K}}} \|\mathbf{X}\|_{2,1}+\frac{\mu}{2}\|P_{\Omega}\mathbf{Z}\|_{2,2}+\frac{\tau}{2}\left\|\mathbf{Z}\text{-}\mathbf{\Psi X}+P_{\Omega}\mathbf{U}+\mathbf{Q}^k/\tau\right\|_2^2 \tag{11}$$

$$\mathbf{Q}^{k+1}=\mathbf{Q}^k+\tau\left(\mathbf{Z}^{k+1}-\mathbf{\Psi X}^{k+1}+P_{\Omega}\mathbf{U}\right) \tag{12}$$

To further simplify the algorithm, we compute $\mathbf{X}^{k+1}$, $\mathbf{Z}^{k+1}$ separately,

$$\mathbf{X}^{k+1}=\arg\min_{\mathbf{W}\in C^{M\times K}} \|\mathbf{X}\|_{2,1}+\frac{\tau}{2}\left\|\mathbf{Z}^k-\mathbf{\Psi X}+P_{\Omega}\mathbf{U}+\mathbf{Q}^k/\tau\right\|_2^2 \tag{13}$$

$$\mathbf{Z}^{k+1}=\arg\min_{\mathbf{Z}\in R^{M\times K}} \frac{\mu}{2}\|P_{\Omega}\mathbf{Z}\|_2^2+\frac{\tau}{2}\left\|\mathbf{Z}-\mathbf{\Psi X}^{k+1}+P_{\Omega}\mathbf{U}+\mathbf{Q}^k/\tau\right\|_2^2 \tag{14}$$

$$\mathbf{Q}^{k+1}=\mathbf{Q}^k+\tau\left(\mathbf{Z}^{k+1}-\mathbf{\Psi X}^{k+1}+P_{\Omega}\mathbf{U}\right) \tag{15}$$

Notice that both Eq. (13) and Eq. (14) have explicit solver. In Eq. (13), using the Parseval's equality in Fourier transform, we have

$$\begin{aligned}\mathbf{X}^{k+1}&=\arg\min_{\mathbf{W}\in C^{M\times K}}\|\mathbf{X}\|_{2,1}+\frac{\tau}{2}\left\|\mathbf{X}^k-\boldsymbol{\Psi}^{-1}\left(\mathbf{Z}+P_{\Omega}\mathbf{U}\right)+\mathbf{Q}^k/\tau\right\|_2^2\\&=S_{1/\tau}\left(\boldsymbol{\Psi}^{-1}\left(\mathbf{Z}^k+P_{\Omega}\mathbf{U}+\mathbf{Q}^k/\tau\right)\right)\end{aligned} \tag{16}$$

$S_{1/\tau}:R^{M\times K}\to R^{M\times K}$ is a shrink operator. Let $\mathbf{W}$ be a $M\times K$ matrix and $\mathbf{w}_j, j=1,\ldots,M$ be rows of $\mathbf{W}$. For each $\mathbf{w}\in C^K$,

$$S_{\mu}(\mathbf{w})=\begin{cases}\left(\|\mathbf{w}\|_2-\mu\right)\dfrac{\mathbf{w}}{\|\mathbf{w}\|_2}, & \text{if}\ \|\mathbf{w}\|_2\geq\mu\\ 0, & \text{otherwise}\end{cases} \tag{17}$$

Then S_{μ} for matrix is defined as:

$$S_{\mu}(\mathbf{W})=\begin{bmatrix}S_{\mu}(\mathbf{w}_1)\\ S_{\mu}(\mathbf{w}_2)\\ \vdots\\ S_{\mu}(\mathbf{w}_M)\end{bmatrix} \tag{18}$$

Direct calculation gives the formula of $\mathbf{Z}^{k+1}$ as follows

$$\mathbf{Z}^{k+1}=\mathbf{W}^{k+1}-\frac{\mu}{\mu+\tau}P_{\Omega}\mathbf{W}^{k+1} \tag{19}$$

where

$$\mathbf{W}^{k+1}=\boldsymbol{\Psi}\mathbf{X}^{k+1}-P_{\Omega}\mathbf{U}-\mathbf{Q}^k/t \tag{20}$$

The algorithm we used to solve the optimization problem Eq. (7) is an iterative algorithm. First, let $\mathbf{Q}^0=\mathbf{Z}^0=0$ and choose a value of τ, then conduct the following iteration until the solution converges:

$$\mathbf{X}^{k+1}=S_{1/\tau}\left(\boldsymbol{\Psi}^{-1}\left(\mathbf{Z}^k+P_{\Omega}\mathbf{U}+\mathbf{Q}^k/k\right)\right) \tag{21}$$

$$\mathbf{W}^{k+1}=\boldsymbol{\Psi}\mathbf{X}^{k+1}-P_{\Omega}\mathbf{U}-\mathbf{Q}^k/k \tag{22}$$

$$\mathbf{Z}^{k+1}=\mathbf{W}^{k+1}-\frac{\mu}{\mu+\tau}P_{\Omega}\mathbf{W}^{k+1} \tag{23}$$

$$\mathbf{Q}^{k+1} = \mathbf{Q}^{k} - \tau\left(\Psi\mathbf{X}^{k+1} - \mathbf{Z}^{k+1} - P_{\Omega}\mathbf{U}\right) \tag{24}$$

3 Field test of a bridge

3.1 Description of the test

The field test on Xiamen Haicang Bridge is carried out. The bridge is a steel box girder suspension bridge with a span distribution of 230m+648m+230m, as shown in Figure 1. The bridge has two tower with height of 140m and the width of the bridge deck is 32m. The test schemes are shown in Figure 2. The tests are repeated 9 times, and the totally test points are 62. Test 1 has seven test points (No. 1-6, and No. 26); wireless sensors are placed on the seven test points to measure the vibration data. After the test is completed, the wireless sensors are moved to the Test 2 which also includes seven test points (No. 7-12 and No. 26). The test point No. 26 is selected as the reference point for all the test. In the same way, the Test 2 to Test 9 are carried out. Nine commercial wireless velocity sensors, as shown in Figure 3, are used in the test, and the sampling frequency for data acquisition is 100Hz.

Figure 1. Xiamen Haicang Bridge

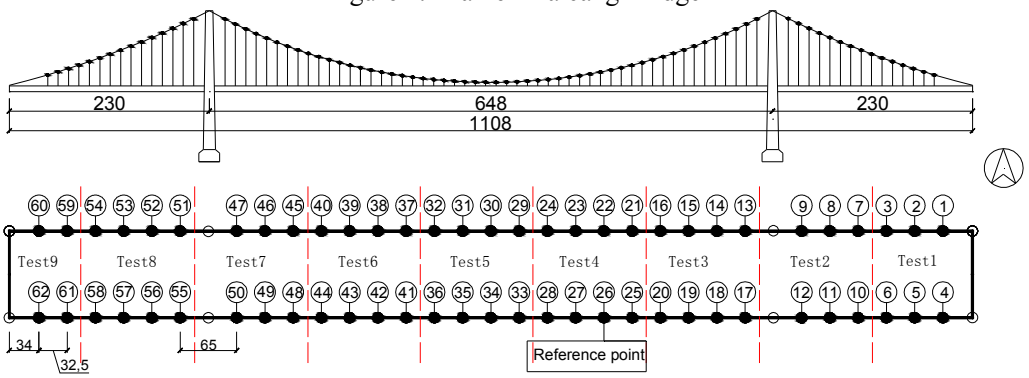

Figure 2. The placement of test points

(a) (b)

Figure 3. The wireless sensor node and wireless base station

The representative dataset measured from the bridge are shown in Figure 4(a). The Fourier spectrum at the measured response are shown in Figure 4(b), which show that the multiple sensors data almost has similar sparsity in the frequency domain. To further illustrate the similar sparsity of multiple sensors data, the cross correlation of the Fourier amplitude spectrum are calculated by:

$$\gamma_{XY} = \frac{\sum_{i=1}^{N}\left(X_i - \bar{X}\right)\left(Y_i - \bar{Y}\right)}{\sqrt{\sum_{i=1}^{N}\left(X_i - \bar{X}\right)^2}\sqrt{\sum_{i=1}^{N}\left(Y_i - \bar{Y}\right)^2}} \tag{25}$$

The results show that the minimal and maximal cross correlation coefficient is 0.5117 and 0.9589, respectively. Most cross correlation coefficients are within a range of [0.7, 0.95]. These cross correlation coefficients further indicate the group sparsity of the signal.

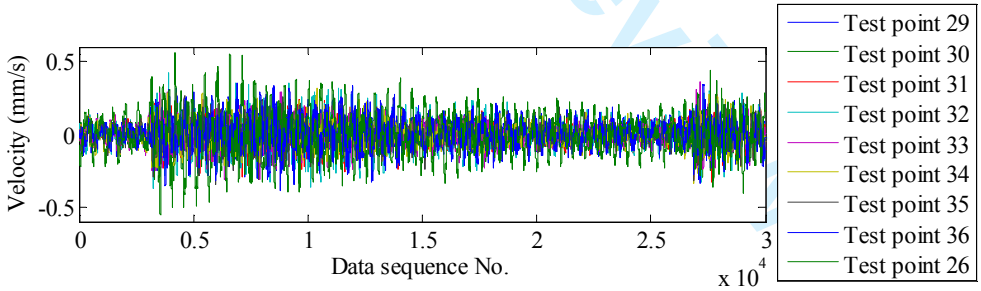

(a) The measured velocity data of test points 29-36 and 26 (the reference point)

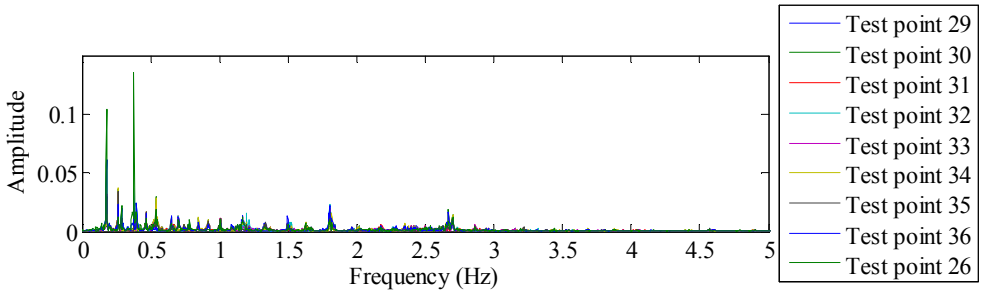

(a) The Fourier specturm of the measured velocity data of test points 29-36 and 26 (the reference point)

Figure 4. The typitical measurements and Fourier specturm

3.2 Data sampling by CS

Since CS sensors are not yet commercially available, the behavior of CS sensors are simulated. The procedure of data sampling by CS is shown in Fig. 5, which shows that the data are random sampled.

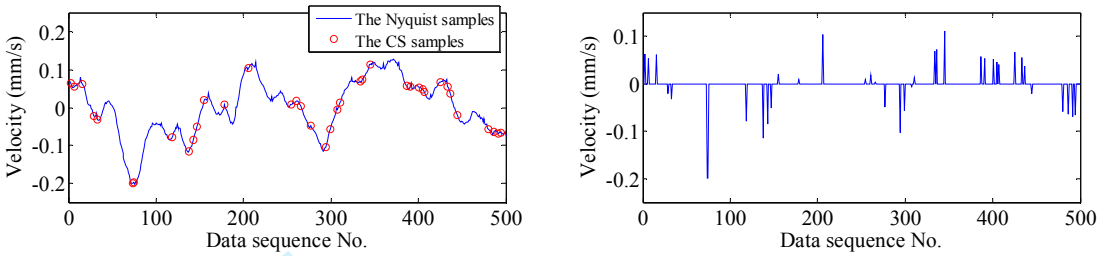

Figure 5. The procedure of data sampling by CS

The typical measured velocity data by wireless sensor is shown in Figure 6(a). We simulate the non-uniform low-rate random sampling of CS, the data with 10%, 20% and 30% samples are shown in Figure 6 (b-d).

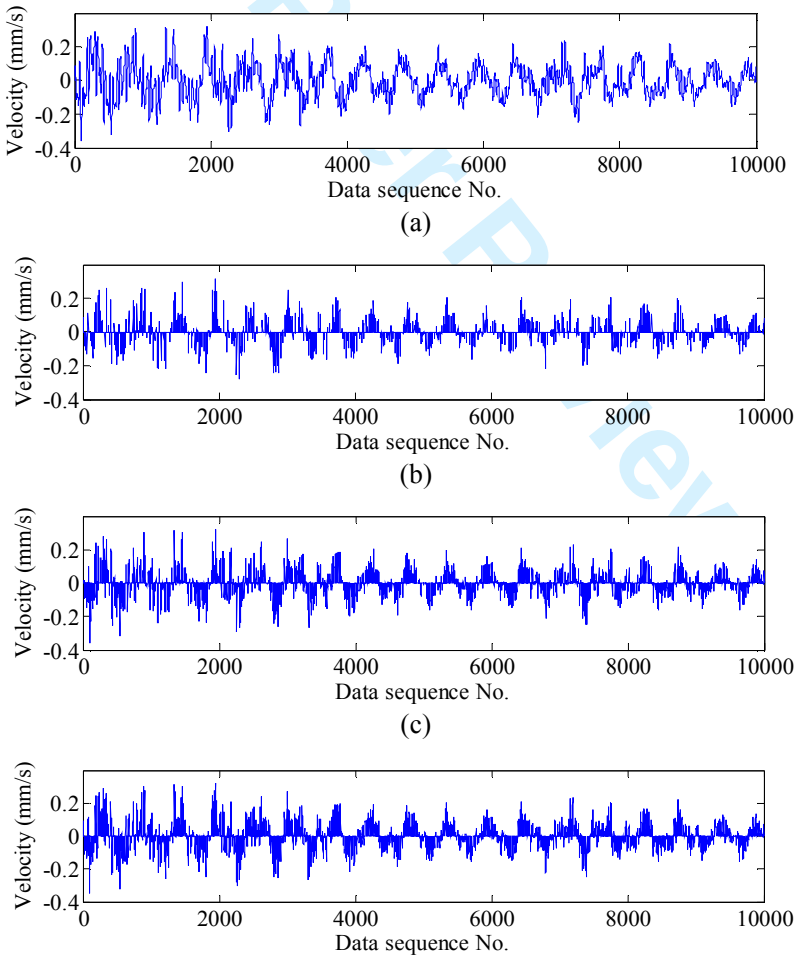

Figure 6. The sampling data by CS: (a) original data; (b) 10% samples; (c) 20% samples; (d) 30% samples

3.3 Data reconstruction results

The data reconstruction results for 10%, 20% and 30% samples are shown in Figures 7-9, respectively. Figures 7(a), 8(a) and 9(a) are the reconstruction results using only one sensor data, and Figures 7(b), 8(b) and 9(b) are the reconstruction results with group sensors data. These figures show that the smaller reconstruction errors can be achieved by considering multiple sensors data using the group sparse optimization methods.

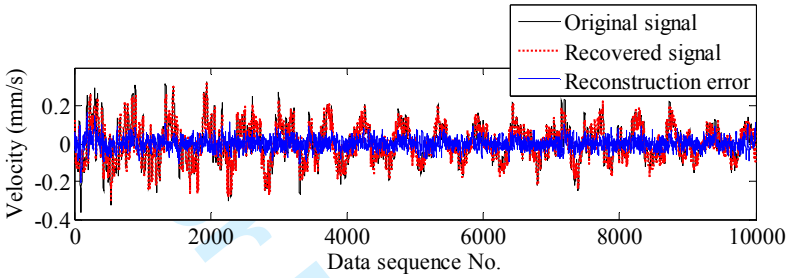

(a)

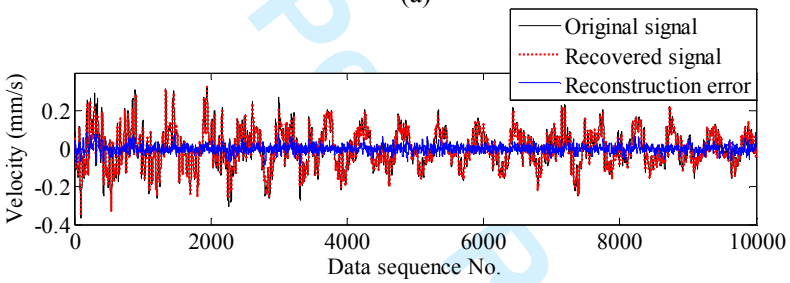

(b)

Figure 7. Data reconstruction results from 10% samples: (a) reconstruction from single sensor data; (b) reconstruction from group sensors data

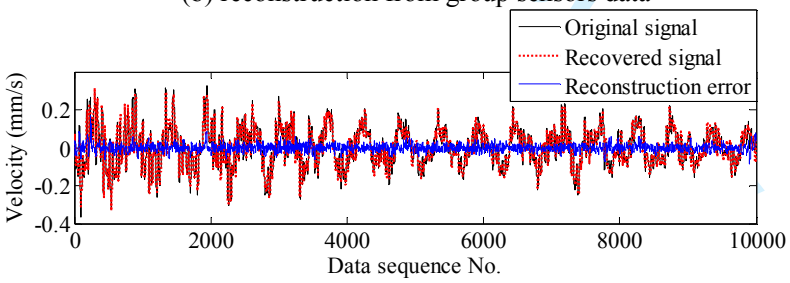

(a)

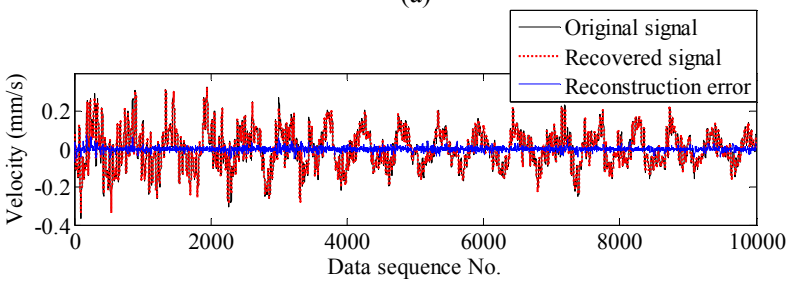

(b)

Figure 8. Data reconstruction results from 20% samples: (a) reconstruction from single sensor data; (b) reconstruction from group sensors data sets

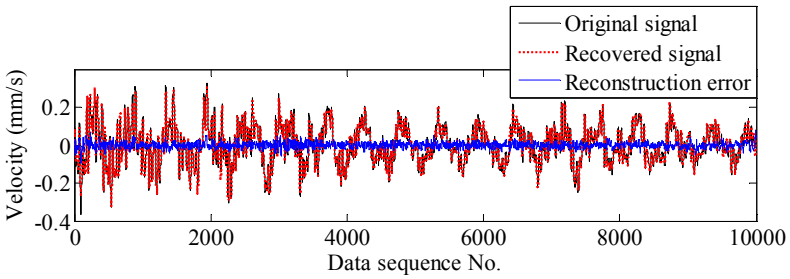

(a)

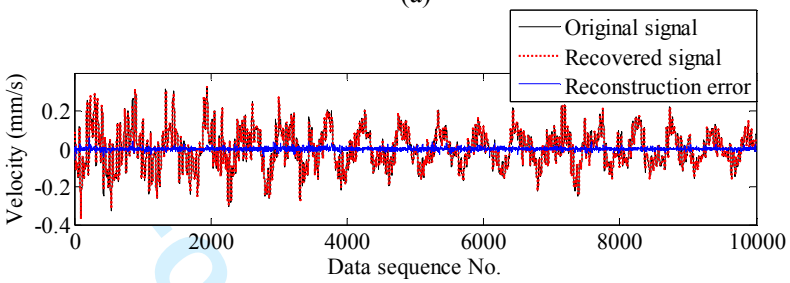

(b)

Figure 9. Data reconstruction results from 30% samples: (a) reconstruction from single sensor data; (b) reconstruction from group sensors data sets

To investigation the relation between sampling ratio and reconstruction error, the sampling ratio 10%, 15%, 20%, 25 % and 30% are considered. The reconstruction error is calculated by

$$\xi = \frac{\left\|\hat{u} - u\right\|_2}{\left\|u\right\|_2} \tag{26}$$

where $\hat{u}$ and u are the reconstruction data and the original data, respectively. The results of data reconstruction error of nine sensors data of Test 5 are shown in Figure 10, showing that the reconstruction errors are decreased with increasing of data sampling ratios for both the single sensor data based and multiple sensors data based group sparse optimization methods. In addition, the reconstruction errors of the multiple sensors data based group sparse optimization method are all less than those of the single sensor data based-optimization method. These further indicate that the group sparsity of multiple sensors data can effectively increase the accuracy of data reconstruction of CS.

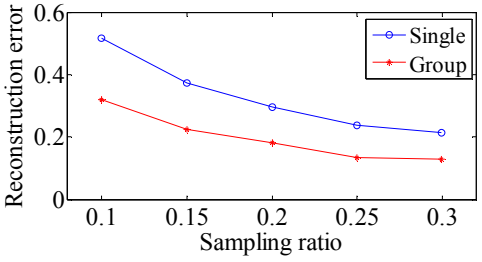

(a) test point 33

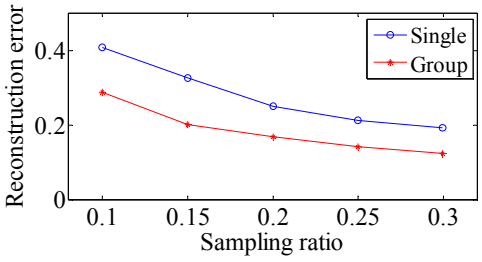

(b) test point 34

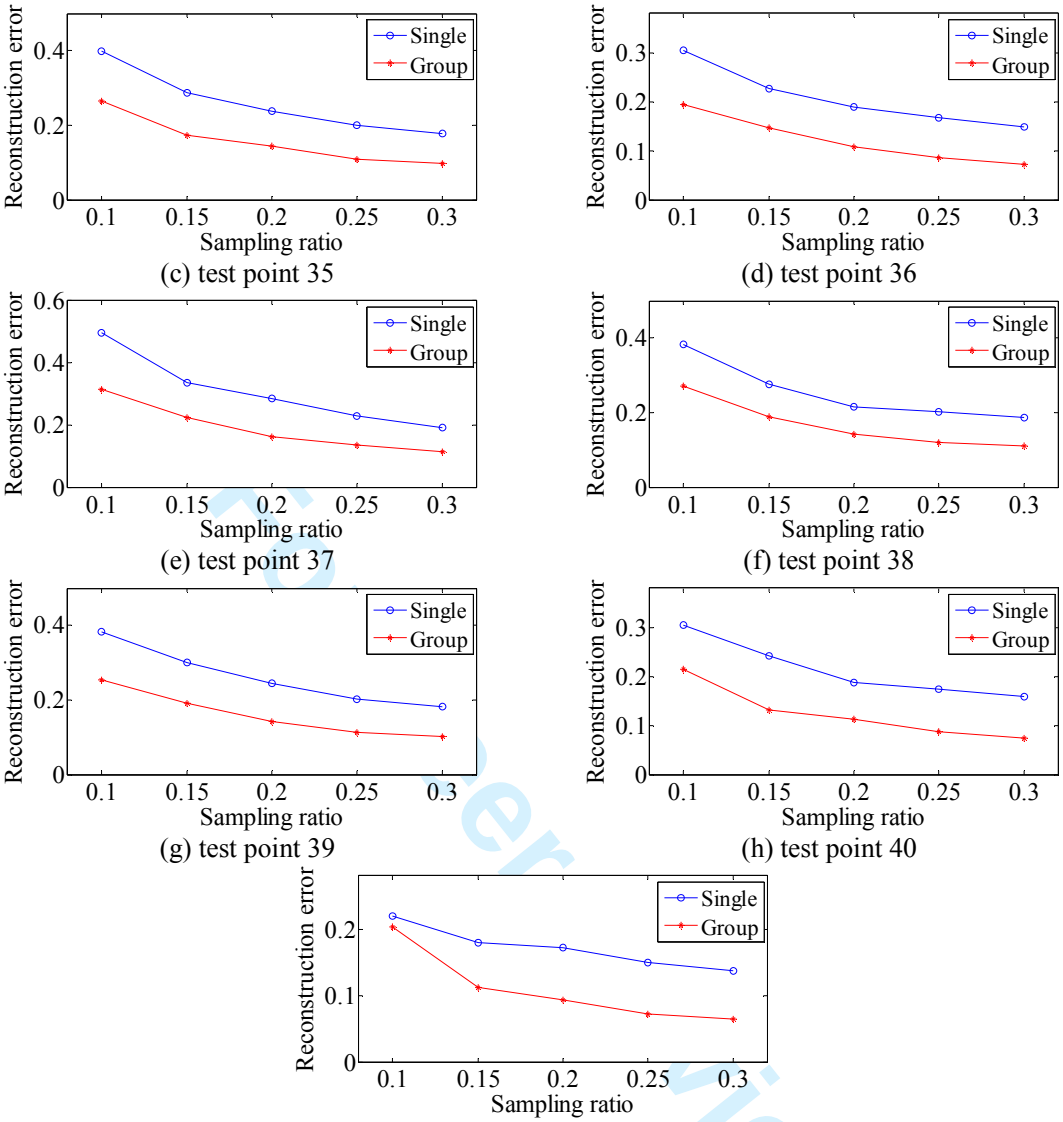

Figure 10. The reconstruction errors with different sampling ratios

The relation of reconstruction error with sensor number used in group sparse optimization based-data reconstruction under different sampling ratio are shown in Figure 11, which shows that the reconstruction error is decreased obviously with increasing of sensor numbers under different sampling ratios from 10%-30%.

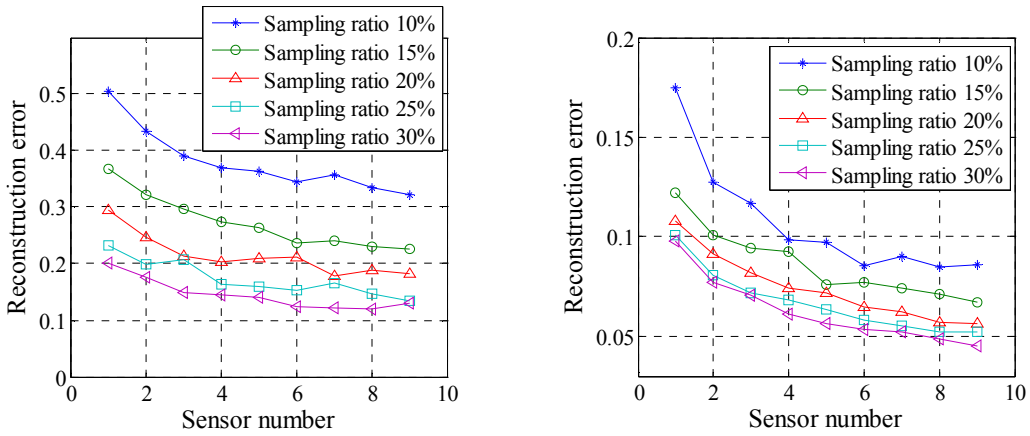

Figure 11. The relation of reconstruction error with sensor number: (a) Test 5; (b) Test 6

The reconstruction errors in time and frequency domain of all test points data are shown in Figure 12 and 13, respectively. These figures show the multiple sensors data based group sparse optimization method obviously decreases the data reconstruction error both in the time and frequency domain. In the case of 10% samples, the minim reconstruction error in all reconstruction data using multiple sensor data based group optimization method is 0.0717, much less than the 0.1401 of single sensor based method. In the case of 30% samples, the minim reconstruction error using multiple sensor data based group optimization method is 0.0344; however the single sensor based method is 0.0826.

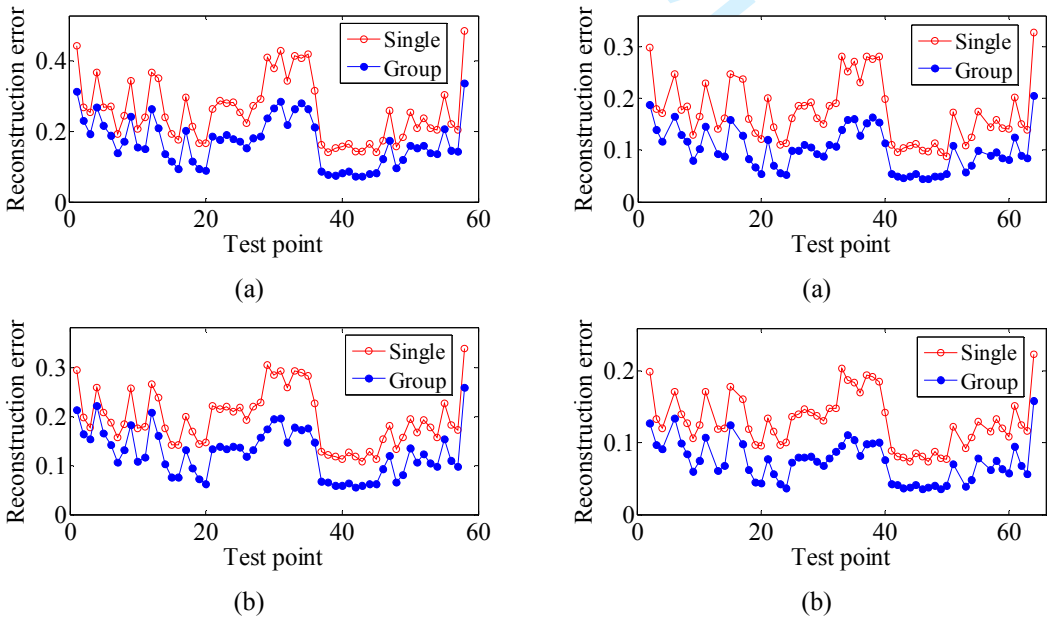

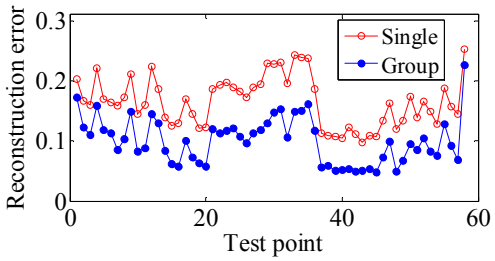

(c)

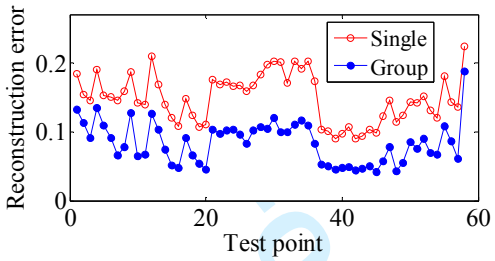

(d)

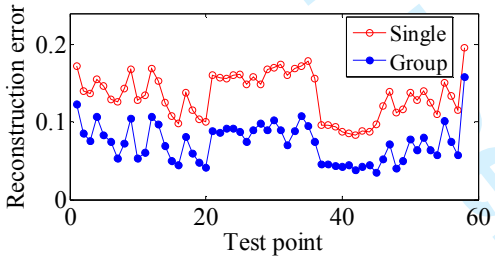

(e)

Figure 12. Reconstruction error in time domain of all test points data: (a) 10% samples; (b) 15% samples; (c) 20% samples; (d) 25% samples; (e) 30% samples;

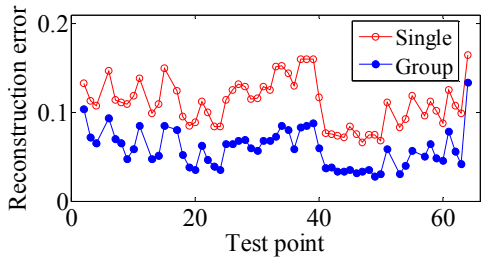

(c)

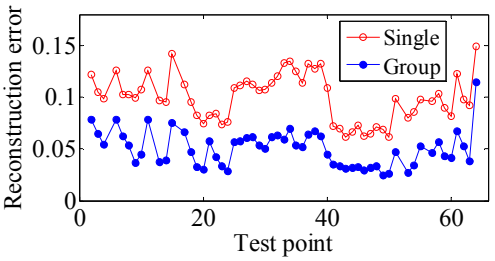

(d)

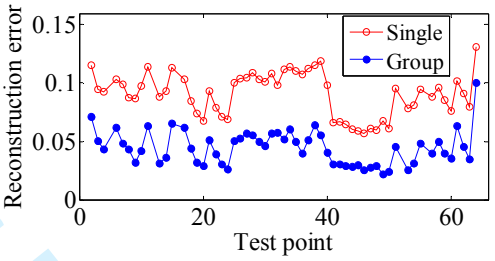

(e)

Figure 13. Reconstruction error in frequency domain of all test points data: (a) 10% samples; (b) 15% samples; (c) 20% samples; (d) 25% samples; (e) 30% samples;

3.3 Modal identification results

The power spectral densities (PSD) of original signal and reconstruction signal with 10% random samples are shown in Figure 14, which shows that PSD results of reconstruction signal from single sensor data and reconstruction signal from group sensors data are very close to those of the original.

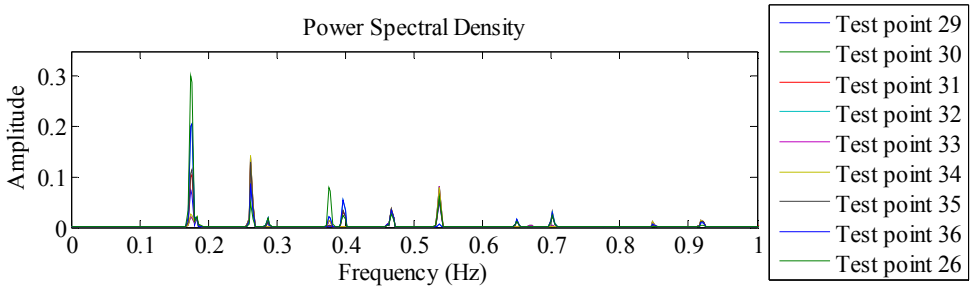

(a)

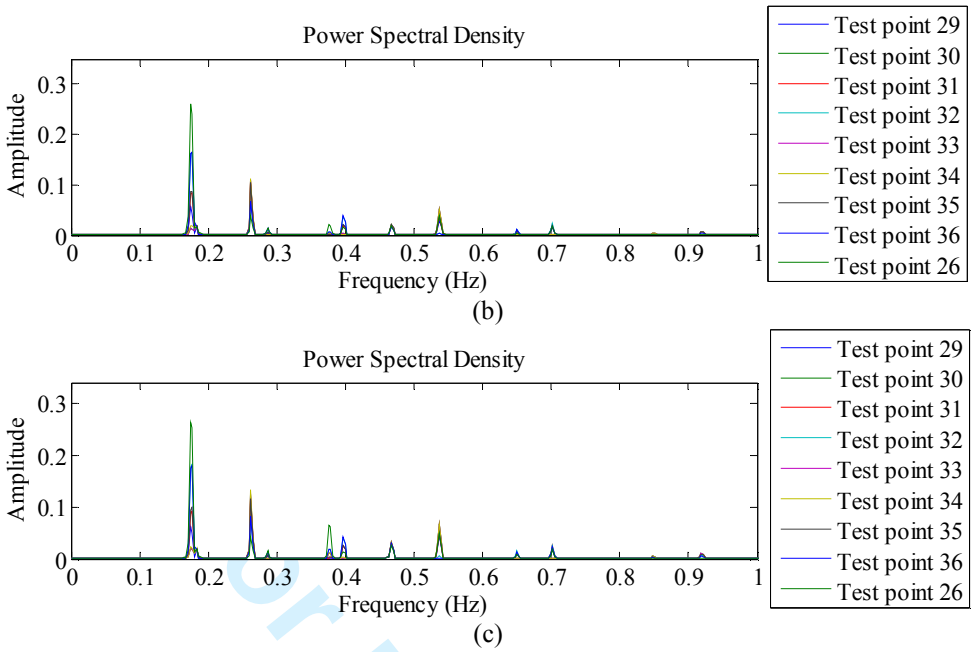

Figure 14. The power spectral densities of the original signal and reconstruction signal: (a) original signal; (b) reconstruction signal from single sensor data with 10% samples; (c) reconstruction signal from group sensors data with 10% samples

To investigate influences of data reconstruction error on the modal identification results, the modal frequencies and mode shapes identified by NExT combined with ERA methods are shown in Tables 1, 2 and Figure 15, respectively. The results show that the identified first two frequencies and mode shapes from reconstruction data are almost consistent with the identification results from original data. This illustrates that the data reconstruction error of the multiple sensors data based-group sparse optimization method and the single sensor data based-optimization method has less impact on modal identification results.

Table 1. Frequency

No.	Theoretical	Identified from original data	Identified from reconstruction data					
			10%		20%		30%	
			Single	Group	Single	Group	Single	Group
1	0.2199	0.2049	0.2033	0.2039	0.2040	0.2034	0.2049	0.2050
2	0.3196	0.2816	0.2835	0.2829	0.2821	0.2822	0.2815	0.2818

Table 2. MAC

No.	Identified from original data	Identified from reconstruction data					
		10%		20%		30%	
		Single	Group	Single	Group	Single	Group
1	0.9877	0.8126	0.8688	0.9671	0.9845	0.9792	0.9808
2	0.9807	0.8428	0.9175	0.8192	0.8690	0.9607	0.9700

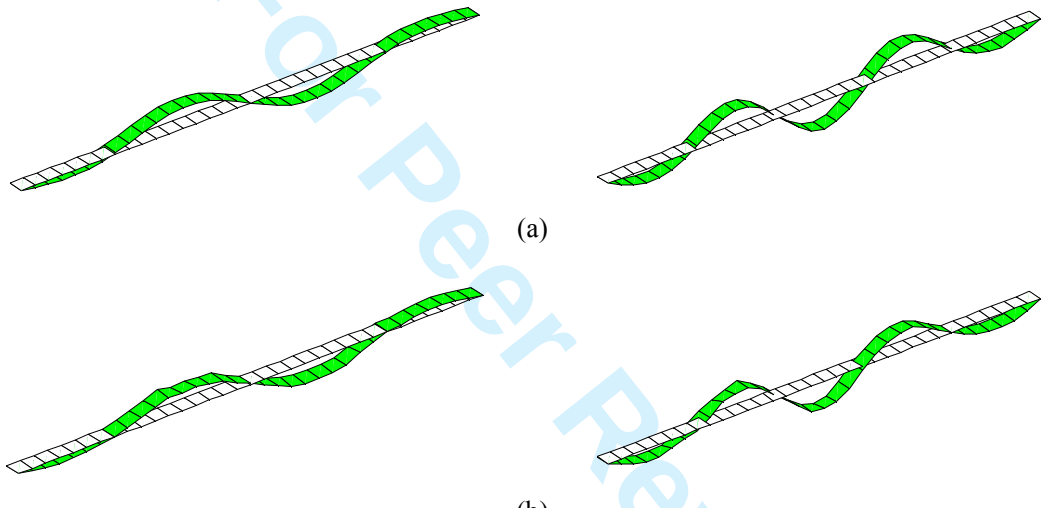

(a)

(b)

Figure 15. The first two identified mode shapes: (a) identificaiton results by original signal; (c) identificaiton results by reconstruction signal from group sensors data with 10% samples

Conclusion

This paper first proposed a group sparse optimization method for compressive sensing data reconstruction of wireless sensors for structural health monitoring, which considers the group sparsity of structural vibration data of multiple sensors on frequency domain to form a data reconstruction optimization problem. Then, the augmented Lagrange multiplier algorithm is employed to solve this optimization problem. Last, the field test results on Xiamen Haicang Bridge by wireless sensors are carried out to verify the proposed method. Some conclusions can be drawn as follows:

(1) The multiple sensors data almost has similar sparsity in the frequency domain. This group sparsity are verified by the cross correlation coefficients, which the values are within a range of [0.7,

0.95]. This indicates that the data has strong correlation in the frequency domain.

(2) The vibration data reconstruction results show that the highly incomplete random sampling data can be well reconstructed using the group optimization method. Even using 10% random sampling data, the original data can be reconstructed by group sparse optimization method with small reconstruction error. Both in time and frequency domain, the reconstruction errors of the multiple sensors data based group sparse optimization method are all less than the single sensor data based-optimization method.

(3) The modal identification results show that the identified frequencies and mode shapes from reconstruction data are almost consistent with the identification results from original data, which indicates that the data reconstruction error of the multiple sensors data based-group sparse optimization method and the single sensor data based-optimization method have less impact on modal identification results.

Acknowledgements

This research was supported by grants from the National Basic Research Program of China (Grant No.2013CB036305), the National Natural Science Foundation of China (Grant No. 51378154, 51678203, 51161120359)

References

1 Ou J and Li H. Structural health monitoring in mainland China: review and future trends, *Struct Health Monit* 2010; 9(3): 219-232.

2 Li H and Ou J. The state of the art in structural health monitoring of cable-stayed bridges. *J Civil Struct Health Monit* 2016; 6(1): 43-67

3 Li HN, Ren L, Jia ZG, et al. State-of-the-art in structural health monitoring of large and complex civil infrastructures. *J Civil Struct Health Monit* 2015; 1-14.

4 Mufti AA. Structural health monitoring of innovative Canadian civil engineering structures. *Struct Health Monit* 2002; 1(1): 89-103.

5 Celebi M. Real-time seismic monitoring of the New Cape Girardeau Bridge and preliminary

analyses of recorded data: an overview. *Earthquake Spectra* 2006; 22(3): 609-630.

6 Straser EG and Kiremidjian AS. A modular visual approach to damage monitoring for civil structures. *Proceedings of SPIE-Smart Structures and Materials*, San Diego, CA, 1996; 2719: 112-122.

7 Lynch JP and Loh KJ. A summary review of wireless sensors and sensor networks for structural health monitoring. *Shock Vib Digest* 2006; 38(2): 91-130.

8 Spencer Jr BF, Jo H, Mechitov KA, et al. Recent advances in wireless smart sensors for multi-scale monitoring and control of civil infrastructure. *J Civil Struct Health Monit* 2016; 6(1): 17-41.

9 Jang S, Jo H, Cho S, et al. Structural health monitoring of a cable-stayed bridge using smart sensor technology: deployment and evaluation. *Smart Struct Syst* 2010; 6(5-6): 439-459.

10 Lynch JP, Wang Y, Loh KJ, et al. Performance monitoring of the Geumdang Bridge using a dense network of high-resolution wireless sensors. *Smart Mater Struct* 2006; 15: 1561-1575.

11 Meyer J, Bischoff R, Feltrin G, et al. Wireless sensor networks for long-term structural health monitoring. *Smart Struct Syst* 2010; 6(3): 263-275.

12 Hoult NA, Fidler PRA, Hill PG, et al. Long-term wireless structural health monitoring of the Ferriby Road Bridge, *ASCE J Bridge Eng* 2010; 15(2): 153-159.

13 Cho S, Giles, RK and Spencer BF. System identification of a historic swing truss bridge using a wireless sensor network employing orientation correction, *Struct Control Health Monit* 2015; 22(2): 255-272.

14 Donoho D. Compressed Sensing. *IEEE Trans Inform Theory* 2006; 52(4): 1289-1306.

15 Candès EJ. Compressive Sampling, *Proceedings of the International Congress of Mathematicians*, Madrid, Spain, August 22-30, 2006.

16 Bao Y, Beck JL and Li H. Compressive sampling for accelerometer signals in structural health monitoring, *Struct Health Monit* 2011; 10(3): 235-246

17 Mascarenas D, Cattaneo A, Theiler J, et al. Compressed sensing techniques for detecting damage in structures. *Struct Health Monit* 2013; 12(4): 325-338

18 Peckens CA and Lynch JP. Utilizing the cochlea as a bio-inspired compressive sensing

technique. *Smart Mater Struct* 2013; 22(10): 105027.

19 O'Connor SM, Lynch JP and Gilbert AC. Compressed sensing embedded in an operational wireless sensor network to achieve energy efficiency in long-term monitoring applications, *Smart Mater Struct* 2014; 23: 085014.

20 Bao Y, Li H, Sun X. et al. Compressive sampling based data loss recovery for wireless sensor networks used in civil structural health monitoring, *Struct Health Monit* 2013; 12(1): 78-95.

21 Zou Z, Bao Y and Li H. Embedding compressive sensing based data loss recovery algorithm into wireless smart sensors for structural health monitoring. *IEEE Sensors Journal* 2014; 15(2): 797-808.

22 Park JY, Wakin MB and Gilbert AC. Modal analysis with compressive measurements. *IEEE Trans Signal Process* 2014; 62(7): 1655-1670.

23 Yang Y and Nagarajaiah S. Output-only modal identification by compressed sensing: Non-uniform low-rate random sampling. *Mech Syst Signal Proc* 2015; 56: 15-34.

24 Wang Y and Hao H. Damage identification scheme based on compressive sensing. *ASCE J Comput Civil Eng* 2013; 29(2): 04014037.

25 Zhou S, Bao Y and Li H. Structural damage identification based on substructure sensitivity and l_1 sparse regularization. *SPIE Smart Structures and Materials+Nondestructive Evaluation and Health Monitoring*, San Diego, California, USA, 10-14 March, 2013

26 Zhou XQ, Xia Y and Weng S. L1 regularization approach to structural damage detection using frequency data. *Struct Health Monit* 2015(14): 6571-582

27 Zhang CD and Xu YL. Comparative studies on damage identification with Tikhonov regularization and sparse regularization. *Struct Control Health Monit* 2016; 23 (3): 560-579.

28 Bao Y, Li H, Chen Z, et al. Sparse l_1 optimization‐based identification approach for the distribution of moving heavy vehicle loads on cable‐stayed bridges. *Struct Control Health Monit* 2016; 23(1): 144-155.

29 Fornasier M and Rauhut H. Recovery algorithms for vector valued data with joint sparsity constraints. *SIAM J Numer Anal* 2008; 46(2): 577-613

30 Mishali M and Eldar YC. Reduce and boost: Recovering arbitrary sets of jointly sparse vectors. *IEEE Trans Signal Process* 2008; 56(10): 4692-4702

31 Tropp JA, Gilbert AC and Strauss MJ. Algorithms for simultaneous sparse approximation, Part I: Greedy pursuit. *Signal Process* 2006; 86: 572-588

32 Tropp JA. Algorithms for simultaneous sparse approximation, Part II: Convex relaxation. *Signal Process* 2006; 86: 589-602.

33 Ming Y and Lin Y. Model selection and estimation in regression with grouped variables. *J R Stat Soc Ser B-Stat Methodol* 2006; 68(1): 49-67